Algorithms for Manifolds and Simplicial Complexes in Euclidean 3-Space

Tamal K. Dey

Dept. of Computer Science
and Engineering
Indian Institute of Technology
Kharagpur 721302
India
e-mail: dey@cse.iitkgp.ernet.in

Sumanta Guha

Dept. of Electrical Engineering
and Computer Science
University of Wisconsin-Milwaukee
Milwaukee, P.O. Box 784, WI 53201
USA
e-mail: guha@cs.uwm.edu

Abstract

A new approach to analyze simplicial complexes in Euclidean 3-space $\mathbf{R}^3$ *is described. First, methods from topology are used to analyze triangulated 3-manifolds in* $\mathbf{R}^3$*. Then it is shown that these methods can in fact be applied to arbitrary simplicial complexes in* $\mathbf{R}^3$ *after (simulating) the process of thickening a complex to a 3-manifold homotopic to it. As a consequence considerable structural information about the complex can be determined and certain discrete problems solved as well.*

For example, it is shown how to determine the homology groups, as well as concrete representations of their generators, for a given complex K*. Further, given a 1-cycle or 2-cycle in* K *it is shown how to express this cycle in terms of the generators of a homology group, which solves the problem of classifying cycles up to their homology class. An application is to the classification of simplicial maps up to their actions on homology groups.*

Recent developments in analyzing molecular structures through a dual simplicial complex, called Delaunay complex, has further enhanced the need for computing structural information about simplicial complexes in $\mathbf{R}^3$*. This paper develops basic techniques to manipulate and analyze structures of complexes in* $\mathbf{R}^3$.

Keywords: Manifolds, surfaces, algebraic topology, knots, links, simplicial complexes, simplicial maps, homology groups, betti numbers, algorithms, computational topology.

1 Introduction

Classification of topological spaces and functions is a primary goal in algebraic topology. The homology groups of a topological space T are invariants that are often computed in order to classify T. Given a continuous function $f : T_1 \rightarrow T_2$ between topological spaces the induced homomorphisms between corresponding homology groups help classify f. It is therefore important not only to compute the homology groups of a topological space, but also a representation of the elements of these groups that in turn allows representation of the induced homomorphisms.

Of particular practical significance are subspaces of Euclidean 3-space $\mathbf{R}^3$. Such subspaces are of course realizable in the real world and, further, the zeroth, first, and second betti numbers (ie. ranks of the corresponding homology groups) have intuitive geometric interpretations as the number of components, tunnels, and voids, respectively. A typical discrete representation of such a subspace is as a simplicial complex embedded in $\mathbf{R}^3$, and of a function is as a simplicial map between complexes.

There is a classical algorithm to compute the homology groups of an arbitrary simplicial complex, see [13], based on reducing certain matrices to a canonical form, called Smith normal form. Unfortunately, the reduction of a matrix to its Smith normal form is a severe computational bottleneck for which the best known algorithm seems to have a worst-case upper bound that is quite a large polynomial in the size of the input [10]. Donald and Chang [5] though contend that most complexes that occur in geometric design, as well as their matrices, are sparse and that the classical algorithm therefore expectedly completes in time quadratic in the size of the complex.

Delfinado and Edelsbrunner [1] describe an algorithm, avoiding the computational bottleneck of reduction to Smith normal form, that computes the betti numbers of a simplicial complex in $\mathbf{R}^3$. Their method is an incremental one that assembles the complex simplex by simplex, and at each step updates the betti numbers of the current complex. It runs optimally in time and space linear in the size of the complex. However, their method does not produce representations of generators of the homology groups, and therefore cannot be further applied to analyze the structure of a simplicial complex or simplicial maps.

We describe here a new approach to analyze complexes in $\mathbf{R}^3$. Our approach is based on first using methods from topology to derive algorithms for a compact triangulated 3-manifold. Because of the relative niceness of compact 3-manifolds in $\mathbf{R}^3$ as topological objects we are able to apply classical results. However, Props. 1-4 that form the basis of our algorithms for 3-manifolds seem not to have appeared as yet in the mathematics literature.

Next we show that these algorithms can apply to simplicial complexes as well, after thickening a given complex to a topological 3-manifold that is homotopic to it, so retaining identical homology. Actually, we simulate such a thickening as we never need to compute an explicit triangulation of the thickened manifold. We describe algorithms to:

1. Determine the ranks of homology groups (betti numbers) of a complex K in $\mathbf{R}^3$ optimally in time and space linear in the size n of K. Although this algorithm is of the same complexity as that of [1] our new insight into the generators of the homology groups allows a somewhat simpler non-incremental algorithm that is different from [1].

2. Compute geometric realizations of a set of generators of the first and second homology groups of K (for the zeroth homology group this is trivial) in $O(n\overline{g})$ and $O(n)$ time (and space), respectively, where $\overline{g}$ is an invariant of K s.t. always $\overline{g} < n$.

3. Given a 1-cycle or 2-cycle of size k in K, compute an expression of the homology class of this cycle in terms of the generators of the corresponding homology group, in $O(n\overline{g}k)$ or $O(n+k)$ time (and space), respectively. This in turn allows to:

   (a) Decide if a cycle is null-homologous, or if two cycles are co-homologous, in other words, classify cycles up to their homology class. A geometric interpretation of a cycle being null-homologous is as follows: roughly, a 1-cycle is null-homologous if it is the boundary of a (2-dimensional) surface in K, while a 2-cycle is null-homologous if it is the boundary of a solid object in K. (See Dey [2] for corresponding results for 2-manifolds.)

   (b) Compute the induced homomorphism of a simplicial map between two complexes, in other words, classify simplicial maps up to their action on homology groups.

It is appealing and instructive how geometric insights often help improve the efficiency of our algorithms. Further, our methods allow more insight into the structure of simplicial complexes in $\mathbf{R}^3$ than earlier ones as geometric realizations of the generators of the first and second homology groups allow "visualization" of tunnels and voids. Consequent applications are probable in such areas as solid modeling, molecular modeling, and alpha-shapes [6, 7, 8, 9].

In molecular biology, for example, homology of structures of polypeptide chains is often examined to determine similarities. An exciting recent development in the work on alpha-shapes is the formalization by Edelsbrunner, Facello, and Liang [8] of the notion of "pockets" or imperfect voids in the three-dimensional structures of macromolecules, which is used in molecular docking. They model the molecules as a union of three-dimensional balls that represent atoms. It is shown in [6, 8] that the space generated by this union is homotopic to a simplicial complex, called the Delaunay complex, which is the dual of the weighted Voronoi diagram of the balls. The definition and the algorithm for pockets are based on this Delaunay complex. Consequently, it is hoped that enhancements in understanding simplicial complexes in R^3 would benefit the computational aspects of molecular structures. For example, initially finding generators of the first homology group could be an approach to determining imperfect tunnels in three-dimensional structures.

In the following we omit all discussion of the prerequisite mathematics that includes elementary algebraic topology, knot theory, and manifold theory. Excellent sources for such material include [13, 15, 16] and we shall point to others as we proceed. However, most of our results are geometrically quite intuitive, and our approach in this version has been to avoid much mathematics in the proofs in favor of intuitive justification.

In Sec. 2 we prove results for 3-manifolds. We show how these results apply to simplicial complexes in Sec. 3. We discuss the complexity of implementation and conclude in Sec. 4.

2 3-manifolds in $\mathbf{R}^3$

We were in fact first motivated by rather elegant algorithms that we found to determine homology groups and their generators for compact 3-manifolds in $\mathbf{R}^3$.

Let M be a compact connected *triangulated* 3-manifold in $\mathbf{R}^3$ (any compact 3-manifold is triangulable, see [12]). Say $M = |K|$, the underlying space of a simplicial complex K. M must necessarily be orientable with non-empty boundary $Bd(M)$, where $Bd(M)$ is a disjoint union of, say, r closed connected orientable surfaces S_i, $1 \leq i \leq r$, of genus g_i, respectively. A triangulation of $Bd(M)$ is obtained as a subcomplex ∂K of K. We shall henceforth often not distinguish between K and M.

At this point it may be useful to give an intuitive description of M. It has an "enclosing" surface, say S_r (adjacent to the unbounded component of the complement of M in $\mathbf{R}^3$); M is then formed from the solid M', bounded by S_r, by excision to form $r-1$ "voids" inside M' that are bounded by the surfaces S_i, $1 \leq i \leq r-1$. The homeomorphic type of M of course depends not only on the S_i but also on their disposition inside S_r, and w.r.t. each other: they may be arbitrarily linked and knotted, see Fig. 1.

Anticipating that when we simulate the thickening of a complex into a 3-manifold we shall only obtain explicit descriptions of the boundary of the thickened manifold, in the following we attempt to compute the homology groups of M and their generators in terms of the bounding surfaces S_i.

Consider a *doubling* of M, the manifold M_d obtained by taking a homeomorphic copy M' of M and identifying corresponding points on their boundaries, see [12, 16]. Then M_d is a compact connected orientable *and closed* (ie. boundaryless) 3-manifold, no longer embeddable in $\mathbf{R}^3$ of course. A triangulation K_d of M_d can be obtained by correspondingly doubling K (or possibly a barycentric subdivision of K [12]).

Now the Euler characteristic of K_d,

$$\chi(K_d) = 2\chi(K) - \chi(\partial K),$$

but the Euler characteristic of a compact closed 3-manifold is 0 by Poincaré duality (see [13]). Therefore,

$$\chi(K_d) = 0 \Rightarrow \chi(\partial K) = 2\chi(K).$$

Further, given the relation between the Euler characteristic and genus of a surface (see [11]),

$$\chi(\partial K) = \sum_{i=1}^{r}(2 - 2g_i) = 2r - 2\sum_{i=1}^{r} g_i.$$

Therefore,

$$\chi(K) = r - \sum_{i=1}^{r} g_i.$$

But Euler's formula gives (see [13]),

$$\chi(K) = \beta_0(K) - \beta_1(K) + \beta_2(K) - \beta_3(K),$$

where the betti number $\beta_i(K)$ is the rank of the homology group $H_i(K)$. We know $\beta_0(K) = 1$ as K is connected, and $\beta_3(K) = 0$ as there exists no non-trivial 3-cycle in $\mathbf{R}^3$. Therefore,

$$\begin{aligned}\beta_1(K) &= 1 + \beta_2(K) - \chi(K)\\ &= 1 + \beta_2(K) - (r - \sum_{i=1}^{r} g_i)\\ &= \sum_{i=1}^{r} g_i + \beta_2(K) - (r-1).\end{aligned}$$

Proposition 1 $\beta_2(K) = r - 1$ *, and the homology classes of the surfaces,* $[S_i], 1 \le i \le r-1$*, generate* $H_2(K)$.

Proof Sketch. The $S_i, 1 \le i \le r-1$, represent $r-1$ independent 2-cycles as they do not bound a 3-chain (a solid object) in K.

Further, any 2-cycle in K is a "sum" of closed connected surfaces. Any such closed surface S must contain some (possibly empty) subset of $\{S_i : 1 \le i \le r-1\}$ in its interior. Say S contains $S_{i_1}, \ldots, S_{i_k}$ in its interior. Then, $[S] = -([S_{i_1}] + \ldots + [S_{i_k}])$, as $S, S_{i_1}, \ldots, S_{i_k}$ together clearly bound a 3-chain (which is the solid object with S as the enclosing surface, and the S_{i_j} bounding voids inside it), so that $[S] + [S_{i_1}] + \ldots + [S_{i_k}] = 0$, with appropriate orientations.

Eg., in Fig. 1, $[S_1] + [S_2] + [S_3] = 0$, as S_1, S_2, S_3 together bound the 3-chain represented by K itself. □

Before considering $H_1(K)$ we need to fix some terminology regarding the generators of the homology group $H_1(S)$ of a closed orientable surface S. If the genus of S is g, then $H_1(S) = \mathbf{Z} \oplus \ldots \oplus \mathbf{Z}$ ($2g$ terms), the free Abelian group of rank $2g$. A set of $2g$ generating cycles of $H_1(S)$ consists of g *latitudinal* and g *longitudinal* generating cycles. This set of $2g$ generating cycles may be computed from a triangulation of S by the method of Vegter and Yap [19]

An intuitive geometric idea of generating cycles may be had by considering a torus embedded in $\mathbf{R}^3$ without any "knotting". See Fig. 2 for an example of a torus of genus 3 in $\mathbf{R}^3$: imagining the inside of the torus to be filled to a solid, we see that exactly 3 of the generators become contractible – these are the latitudinal generators. However, distinction between latitudinal and longitudinal generators may not be quite so simple if a surface is embedded with knots and links (we do not as yet formalize the notions of knotting and linking) as, eg., in Fig. 1. A surface in $\mathbf{R}^3$ is either a sphere or sum of tori, and each torus is constructed by rotating one generator along another generator. Any of these two generators may be a knot in $\mathbf{R}^3$, so producing knotted surfaces. Further, different tori may be linked with one another. We defer consideration of how, in fact, to generally distinguish between longitudinal and latitudinal generators to later in this section.

Proposition 2 $\beta_1(K) = \sum_{i=1}^{r} g_i$. *Let* $C^i_{L,1}, \ldots C^i_{L,g_i}$ *and* $C^i_{l,1}, \ldots, C^i_{l,g_i}$ *be* g_i *latitudinal and longitudinal generating cycles of* S_i*, respectively,* $1 \le i \le r$.

Then, the set of $\sum_{i=1}^{r} g_i$ *homology classes of cycles*

$$X = \cup_{i=1}^{r-1} \{[C^i_{L,1}], \ldots [C^i_{L,g_i}]\} \cup \{[C^r_{l,1}], \ldots, [C^r_{l,g_r}]\}$$

forms a basis of $H_1(K)$.

Proof Sketch. The first equation follows from Eqn. 1 and Prop. 1.

Recall that $M = |K|$ with the outer surface S_r and inner surfaces $S_i, i = 1, \ldots, r-1$. Let $L = S_1 \cup S_2 \ldots \cup S_r$. Observe that any closed surface S in $\mathbf{R}^3$ divides $\mathbf{R}^3$ into two disjoint open connected components, denoted C_S and C'_S, such that $C_S \cup C'_S \cup S = \mathbf{R}^3$, $Bd(C_S) = Bd(C'_S) = S$, and C_S is bounded while C'_S is unbounded.

Let M' be another compact 3-manifold (not necessarily connected) which is formed as follows. Consider embeddings of the surfaces S_i, $i = 1, 2, \ldots, r$ in $\mathbf{R}^3$ *without* any knotting or linking. Let S'_i denote the newly embedded surface S_i, where $S'_1, S'_2, \ldots, S'_{r-1}$ are assumed embedded in $C_{S'_r}$. Define M' by

$$M' = (C_{S'_1} \cup C_{S'_2} \ldots \cup C_{S'_{r-1}}) \cup (C'_{S'_r}) \cup (S'_1 \cup S'_2 \ldots \cup S'_r) \cup p_\infty,$$

where p_∞ denotes the point at infinity.

Informally, M' is obtained by filling the inside of surfaces $S'_1, S'_2, \ldots, S'_{r-1}$, which are homeomorphic to $S_1, S_2, \ldots, S_{r-1}$, respectively, and are without any knotting or linking, and then filling the outside of surface S'_r, which is homeomorphic to S_r, together with a single point compactification at infinity. The compact manifold M' can be thought of as a complement of M, but without any knotting or linking among its bounding surfaces.

It may be shown that the latitudinal generators of $S'_1, S'_2, ..., S'_{r-1}$ and the longitudinal generators of S'_r form a basis of $H_1(M')$. We omit details here. A natural extension of this approach for the manifold M faces difficulty due to the possible knotting and linking of its surfaces. To overcome this we proceed as follows. Take the union of M and M' and then identify $Bd(M)$ and $Bd(M')$ to create the space, denoted T, where this identification uses the homeomorphisms $h_i : S_i \rightarrow S'_i$, for $i = 1, ..., r$, such that h_i takes latitudinal and longitudinal generators of S_i to the latitudinal and longitudinal generators of S'_i respectively. Certainly T is a compact 3-manifold without boundary, and hence has Euler characteristic $\chi(T) = 0$ by Poincaré duality. It can be proved that the second homology group of T, i.e. $H_2(T)$, is trivial giving $\beta_2(T) = 0$. We omit a formal proof of this fact in this version. Also $\beta_0(T)$ and $\beta_3(T)$ are both 1 since there is only one component in T, and only one generator, namely T itself, for 3-cycles. Since $\chi(T) = 0 = \beta_0(T) - \beta_1(T) + \beta_2(T) - \beta_3(T)$, we have $\beta_1(T) = 0$. Hence, $H_1(T)$ is trivial as well.

Now $L = M \cap M'$ after identification. Observe that L is the union of the set of tori that constitute $Bd(M) = Bd(M')$. The following piece of the Mayer-Vietoris sequence of (M, M') is exact (see [13] for relevant definitions):

$$H_2(T) \rightarrow H_1(L) \xrightarrow{\phi} H_1(M) \oplus H_1(M') \rightarrow H_1(T).$$

As $H_1(T)$ and and $H_2(T)$ are both trivial, the following is exact,

$$0 \rightarrow H_1(L) \xrightarrow{\phi} H_1(M) \oplus H_1(M') \rightarrow 0,$$

so that ϕ is an isomorphism. As a result, a basis of $H_1(L)$ must be split into two parts such that one part is mapped to a basis of $H_1(M)$ and the remainder is mapped to a basis of $H_1(M')$ by ϕ in a one-to-one manner. The isomorphism ϕ respects the homeomorphisms h_i between $Bd(M)$ and $Bd(M')$ used for identification. Consequently, ϕ maps the latitudinal generators of $S_1, S_2, ..., S_{r-1}$ and the longitudinal generators of S_r to the latitudinal generators of $S'_1, S'_2, ..., S'_{r-1}$ and to the longitudinal generators of S'_r, respectively, which form a basis of $H_1(M')$. This implies that ϕ maps the remaining generators in L, i.e. the longitudinal generators of $S_1, S_2, ..., S_{r-1}$ and the latitudinal generators of S_r, to a basis of $H_1(M)$. It follows, therefore, that

$$X = \cup_{i=1}^{r-1} \{[C^i_{L,1}], \ldots [C^i_{L,g_i}]\} \cup \{[C^r_{l,1}], \ldots, [C^r_{l,g_r}]\},$$

forms a basis of $H_1(M)$.

Figs. 3 and 4 illustrate this proposition for different cases. In Fig. 3 the surfaces S_i are not knotted or linked. In such cases the latitudinal generators of the $S_i, 1 \leq i \leq r-1$, and the longitudinal generators of S_r are not null-homologous (identity in $H_1(K)$), while the remaining generators are null-homologous. Eg., in Fig. 3 it is easy to imagine the longitudinal generators of S_1 and S_2 and the latitudinal generator of S_3 each bounding a distinct disc in K (in fact, Seifert surfaces [15], on which each can "contract" to a point), while the other 3 generators do not. The homology classes of generators that are not null-homologous form a basis of $H_1(K)$.

Even if the S_i are knotted and linked the second part is seen to be true after some reflection. Eg., consider Fig. 4(a) where the torus S_1 "winds" twice through torus S_2. No longer is $C^2_{l,1}$ null-homologous, but $[C^2_{l,1}] = 2[C^1_{L,1}]$, as a disc bounded by $C^2_{l,1}$ is punctured twice by cycles homotopic to $C^1_{L,1}$. Thus, despite the linking, $\{[C^1_{L,1}], [C^2_{L,1}], [C^3_{l,1}]\}$ is still a basis of $H_1(K)$.

In Fig. 4(b) neither $C^1_{l,1}$ nor $C^2_{L,1}$ is null-homologous, but $[C^1_{l,1}] = [C^2_{l,1}]$ and $[C^2_{L,1}] = [C^1_{L,1}]$, as one can imagine two annular strips in K, one bounded by $C^1_{l,1}$ and $C^2_{l,1}$, and the other by $C^2_{L,1}$ and $C^1_{L,1}$, so that these pairs of cycles are co-homologous, respectively (one cycle can "transform" to the other of the pair along the annulus). Thus, $\{[C^1_{L,1}], [C^2_{l,1}], [C^2_{l,2}]\}$ is a basis of $H_1(K)$. □

Now that we have succeeded in determining geometric realizations of sets of generators of $H_1(K)$ and $H_2(K)$, we proceed to the problem of determining for a given 1-cycle or 2-cycle in K an expression in terms of these generators.

For a 2-cycle in K represented by a surface S the following is an easy consequence of the method of proof of Prop. 1:

Proposition 3 *Given a surface S in K, $[S]$ is the negative of the sum of those $[S_i]$ (from $[S_1], \ldots, [S_{r-1}]$) such that S_i is contained in the interior of S.* □

Before considering 1-cycles in K we need to formalize the notion of the *linking number* $L(C_1, C_2)$ of two disjoint oriented polygonal knots C_1 and C_2 in $\mathbf{R}^3$. Intuitively, $L(C_1, C_2)$ counts the number of times one of C_1 and C_2 winds through the other. We give below two equivalent definitions (from [15]); the first one should motivate the next proposition, while the second suggests a method to compute the linking number:

1. As $H_1(\mathbf{R}^3 - C_2) = \mathbf{Z}$, the integers, [15], we can choose a generator $[C']$ of this group (in fact C' may be chosen to be a latitudinal generating cycle of a tubular toroidal neighborhood of C_2). Then, if the homology class $[C_1] = n[C']$ in $H_1(\mathbf{R}^3 - C_2)$, define $L(C_1, C_2) = n$.

2. Consider a *regular* projection π of $C_1 \cup C_2$ on to a plane P that is below both C_1 and C_2. (pro-

jection $\pi : C_1 \cup C_2 \to P$ is regular if $|\pi^{-1}(p)| \leq 2, \forall p \in P$). For each point $p \in P$ at which $\pi(C_1)$ intersects $\pi(C_2)$, *and* where C_1 crosses *under* C_2 (above p), assign a crossing number of ± 1 according to the orientation of the crossing, see Fig. 5(a). If the sum of all crossing numbers at intersection points on P (assign a crossing number of 0 if C_1 crosses above C_2) is n, define $L(C_1, C_2) = n$.

Eg., in Fig. 5(b) (unfortunately on paper we can *only* depict projections and not the curves in 3-space!) $L(C_1, C_2) = 2$.

Proposition 4 *Given a 1-cycle C in the interior of K that is an embedding of S^1 (in other words, a polygonal knot: all 1-cycles in K are sums of such knots), $[C]$ is a linear sum of the homology classes of the generating cycles as follows,*

$$[C] = \sum_{i=1}^{r-1} \sum_{k=1}^{g_i} a_k^i \, [C_{L,k}^i] \; + \; \sum_{k=1}^{g_r} a_k^r \, [C_{l,k}^r],$$

where,

$$a_k^i = L(C, C_{l,k}^i), \; 1 \leq i \leq r-1, \; 1 \leq k \leq g_i, \; and,$$

$$a_k^r = L(C, C_{L,k}^r), \; 1 \leq k \leq g_r.$$

Simply, the coefficient, in the above sum, of a latitudinal (longitudinal) generating cycle is the linking number of C and the corresponding longitudinal (latitudinal) cycle. Note. The linking numbers are well-defined as C, which is in the interior of K, is disjoint from the generating cycles. We discuss later how to (a) choose appropriate orientations on the generating cycles, and (b) deal with the case when C does not lie in the interior of K.

Proof Sketch. First we give intuitive justification. Consider the simple situation shown in Fig. 6(a). Here $L(C, C_{l,1}^1) = 1$, $L(C, C_{l,1}^2) = -1$ and $L(C, C_{L,1}^3) = 0$, and it is clear that indeed $[C] = [C_{L,1}^1] - [C_{L,1}^2]$, by observing that a disc bounded by C is punctured once each by cycles homotopic to $C_{L,1}^1$ and $C_{L,1}^2$, respectively.

In Fig. 6(b) $L(C, C_{l,1}^1) = L(C, C_{L,1}^2) = 1$, and considering that an annular strip bounded by C and $C_{l,1}^2$ is punctured by a cycle homotopic to $C_{L,1}^1$ confirms that $[C] = [C_{L,1}^1] + [C_{l,1}^2]$.

A general proof can be based on an inductive application of the first definition of the linking number given above, which we omit here. □

A couple of questions arise (that may already have occurred to the reader):

1. Given a set of $2g_i$ generating cycles of the surface S_i, computed eg. by the method of Vegter and Yap [19], how do we distinguish between latitudinal and longitudinal ones? Recall that we do not necessarily have a triangulation of the ambient space, ie. any information about the disposition of S_i w.r.t. the rest of $\mathbf{R}^3$.
2. The first question in fact leads to asking, given an embedding of K, how do we decide which of the bounding surfaces is the enclosing surface S_r (moreover, can we decide which is the "interior" of a given bounding surface)?

Let us resolve the second question first. For this shoot a ray $\vec{r}$ in an arbitrary direction from a point on any surface S_i. In linear time compute all intersection points along $\vec{r}$ with surfaces S_i. The last intersection point along $\vec{r}$ must necessarily be due to S_r, thus identifying the outer surface.

However, a geometric insight allows us to avoid altogether shooting rays to detect the enclosing surface, and to implement Prop. 3 in linear time. To understand this first consider an analogous situation in $\mathbf{R}^2$ depicted in Fig 7, where *either* bounding circle C_1 or C_2 may be embedded as the "enclosing" circle of the annulus A, and the two embeddings vary by a homeomorphism of a neighborhood of A in $\mathbf{R}^2$. This suggests, in the situation of Prop. 3, to simply "designate" any one bounding surface as the enclosing surface S_r, and designate that side of S to be interior that does not contain S_r. Observe that we can distinguish the two sides of S (which splits K into two connected components), and the surfaces S_i contained in either, by a simple linear time search.

Another geometric insight helps us resolve the first question. We introduce the method of *barycentric perturbation*:

For each surface S_i, construct the generators $C_{L,k}^i$ and $C_{l,k}^i$ in longitudinal/latitudinal pairs by the method of Vegter and Yap [19, Lemma 4.3]. For each $k = 1, ..., g_i$, this method produces the pair of cycles $C_{L,k}^i$ and $C_{l,k}^i$ intersecting at a single point, and such that cycles from distinct pairs do not intersect. To distinguish the latitudinal and longitudinal generators in a pair, we construct the first barycentric subdivision K' of K [13]. Consider the longitudinal generating cycle $C_{l,k}^i$. If $C_{l,k}^i$ is *perturbed in K', minimally* to avoid intersecting $C_{L,k}^i$ in K', then it is geometrically evident that the linking number of $C_{l,k}^i$ (after perturbation) and $C_{L,k}^i$ is 0. See Fig. 8. However, if a latitudinal generating cycle $C_{L,k}^i$ is similarly minimally perturbed in K', the linking number of $C_{L,k}^i$ and $C_{l,k}^i$ becomes ± 1. Choose orientations of the generating cycles so that this linking number in fact becomes 1.

The situation is symmetric for the enclosing surface S_r. A longitudinal generating cycle of a pair perturbs to link (with linking number ± 1) with the other generating cycle, while the latitudinal generating cycle does not link with the other generating cycle after minimal perturbation.

Next, consider the problem of computing linking numbers in Prop. 4 when the given 1-cycle C does not lie in the interior of K, but in fact intersects at least one generating cycle. The solution of course is to minimally perturb C in K' so that it avoids intersections.

We should remark that the reason to go to the first barycentric subdivision K' to perform perturbations is that it is just fine enough that we can perturb (homotopically) a 1-cycle C to avoid intersections it originally had in K without causing a new one.

To sum up we answer the first question as follows: If we know the enclosing surface S_r (after say ray-shooting) then we can distinguish latitudinal and longitudinal generating cycles using above ideas. Interestingly, even without finding S_r (and thereby saving complexity), we can, using the similar ideas, compute *some* generating set of cycles for K: consider each bounding surface in turn, compute a set of its generating cycles in pairs, minimally perturb each cycle of every pair in turn, and retain (with appropriate orientations) exactly those that link non-trivially with the other generating cycle of that pair after perturbation (of course, we do not know which is latitudinal or longitudinal!).

Comment. Another interesting insight suggests that, even if we did not proceed as above to find a basis of generating cycles, it would nevertheless be possible to classify 1-cycles up to a homology class. The reason is that any cycle in K *cannot* link non-trivially with a latitudinal (longitudinal) generating cycle of an inside (outside) bounding surface, as it would have to "leave" K to do so: thus a cycle is null-homologous exactly when it links trivially with *every* generating cycle of *all* the bounding surfaces. This idea will subsequently help improve the implementation of our algorithms.

Simplicial Maps

Now that we can compute an expression of an arbitrary 1- or 2-cycle in the triangulation K of a 3-manifold M in term of the generators of the first and second homology groups of M, it is possible to investigate a simplicial map $f : K_1 \rightarrow K_2$ between the triangulations of two 3-manifolds:

Compute sets of generators of $H_1(K_1)$ and $H_2(K_1)$. Determine the images of these generators in K_2 under f (f takes 1-cycles to 1-cycles and 2-cycles to 2-cycles), and compute an expression of these images in terms of generators of $H_1(K_2)$ and $H_2(K_2)$. This classifies f up to the homomorphism it induces on homology groups.

Further Analysis of the Structure of a 3-Manifold

As we remarked earlier the homeomorphic type of a 3-manifold M in $\mathbf{R}^3$ depends not only on the bounding surfaces S_i but also on the knotting and linking of these surfaces. Once we have determined the bounding surfaces S_i and computed sets of generating cycles for each, more information may be derived about the structure of M by computing linking numbers of various pairs of generating cycles of different S_i. This gives information about the disposition of the voids bounded by the S_i w.r.t. each other, eg. for a manifold as in Fig. 1.

3 Simplicial Complexes in $\mathbf{R}^3$

A triangulated object K in $\mathbf{R}^3$ may of course not be a manifold. It may have both 1-dimensional and 3-dimensional *parts* while its 2-dimensional part may be "honeycombed", see Fig. 9(a): the collection of d-simplexes of K that are not a face of any $(d+1)$-simplex of K, together with all faces of such d-simplexes, constitutes a subcomplex $K' \subseteq K$, called the d-dimensional part of K. In this section we show how K may be thickened to a 3-manifold M that is homotopic to K, so that the results for 3-manifolds of the previous section can apply to analyze the structure of K, as well as analyze simplicial maps between two such complexes K_1 and K_2. Our discussion will be somewhat informal but hopefully we will convince the reader of the validity of our procedure.

First, we note that for ease of presentation we shall excise 1-(and 0-)dimensional parts of K as necessary. These parts are graphs that are structurally simple to handle and we can either (a) deal with them separately, or (b) thicken each graph to a tubular neighborhood and attach back after thickening the remainder of K. See Fig. 9(b).

A *hive* is defined to be an at most 3-dimensional simplicial complex where every 1-simplex is the face of *two or more* 2-simplexes (ie. triangles). An edge e of a triangle t of a simplicial complex is said to be *bare* if it is only a face of t and no other triangle. A triangle is said to be bare if it has at least one bare edge. Thus a hive is an at most 3-dimensional complex with no bare triangles. Intuitively, a hive is a "closed multi-chambered" object.

Fig. 10 indicates a scheme to homotopically transform a complex K without 1(*or* 0)-dimensional parts into a hive H by systematically removing bare triangles.

Now, it should be intuitively clear that a hive H can be thickened to a 3-manifold M homotopic to it. We shall see that the process of thickening may in fact be "simulated" without computing an explicit triangulation of M.

Consider a triangle t of H and choose a vector $\vec{n}$ normal to t (ie. a choice of a side of t), such that t is not the face of a tetrahedron on that side. Imagine thickening t by the width of a small ϵ in the direction of $\vec{n}$. For each edge e_i of t, $i = 1, 2, 3$, find the triangle t_i with e_i as edge that is adjacent to t by rotation around e_i in the direction $\vec{n}$. As H is a hive such t_i exist, and as the embedding of H in $\mathbf{R}^3$ is assumed known, each t_i may be found by a search through the linked list of triangles adjacent to e_i.

Now, imagine thickening each t_i correspondingly by a width of ϵ on the side that it is struck by the rotation around e_i as described above. We may continue this procedure at the remaining borders of the t_i, and further on through H in a breadth-first manner.

Finally, we shall indeed have a thickening of H to a 3-manifold M such that each bounding surface of M retracts homotopically on to a surface represented by a connected component of the graph G whose vertices are pairs $(t, \vec{n})$, where t ranges over triangles that do not face tetrahedrons on both sides and the $\vec{n}$ (at most 2 per t) indicate the sides of t not facing a tetrahedron. Adjacencies of vertices in G are defined as above (a later version of [1] considers a similar graph as well). Thus, if T is a triangulation of M then we immediately have an explicit triangulation ∂T of the boundary $Bd(M)$ of M.

Note though that we have avoided discussing certain subtleties in the thickening procedure that arise, eg., when two surfaces meet at a single a vertex.

Computing betti numbers and generators

In fact it may be seen that $\chi(\partial T) = 2\chi(H)$ which, following the formulae in Sec. 2, implies that $\sum_{i=1}^{r} g_i = r - \chi(H)$, where r is the number of bounding surfaces (= number of components of G) and the $g_i, 1 \leq i \leq r$, are the genus of the bounding surfaces.

Thus after detecting all S_i, it is a matter of simple simplex counting in H to determine $\Sigma_{i=1}^{r} g_i$ and hence the betti number β_1 by Prop. 2. The number of S_i's determine the second betti number β_2 by Prop. 2. This eliminates the 1-cycle detection step entirely from the algorithm of [1]. Further, Props. 1 and 2 may also be applied to compute a representation of the generators of $H_1(H)$ and $H_2(H)$.

Application of Prop. 3 to express a 2-cycle in terms of generators of $H_2(H)$ is straightforward as well. However, application of Prop. 4 requires a little care in that after the projection of a generating cycle of M and a cycle in H on a plane, it should be taken into account, when deciding the crossing number at an intersection, that the generating cycle is a small distance away in a known direction (thus allowing determination of the orientation at each crossing) from triangles of H.

Comment. We need not have excised 1-(and 0-)dimensional parts or transformed to a hive before thickening, but it seems in fact more intuitive and convenient to describe the thickening of a hive.

4 Complexities and Conclusions

We assume that the triangulated manifold or complex is represented in a practical data structure, eg. as the one described in [9]. The only non-standard subroutines that are required to implement our algorithms are to:

1. *Compute the first barycentric subdivision and perform barycentric perturbation of a cycle.*

   The first barycentric subdivision is easily checked to be an $O(n)$ time and space procedure given a triangulation of size n. Minimally perturbing a cycle of length k requires essentially to traverse it edge by edge, incurring $O(1)$ cost to avoid each intersection, for a total of $O(k)$ time and space.

2. *Compute the $2g$ generators of a triangulated surface S_i.*

   For this we invoke the algorithm of Vegter and Yap [19, Th. 4.2] that runs in time and space $O(g_i n_i)$, where the triangulation of S_i is of size n_i and g_i is its genus (for a total complexity of $O(n\overline{g})$ for r surfaces, where $\sum_{i=1}^{r} n_i = O(n)$ and $\overline{g} = \max_{1 \leq i \leq r} g_i$).

3. *Compute the the linking number of two disjoint oriented polygonal knots C_1 and C_2 in $\mathbf{R}^3$.*

   Assume C_1 and C_2 are of lengths k_1 and k_2, respectively. Project the knots in linear time on an arbitrary plane (if the projection is not regular it can be perturbed slightly to regularize) to obtain two closed polygonal curves C_1' and C_2' of lengths k_1 and k_2, respectively, on the plane. Compute all intersections of C_1' and C_2' using even the naive algorithm in $O(k_1 k_2)$ time and space (*any* algorithm would have a similar worst-case because of output size [14]). It is then possible to determine in constant time per intersection point p the crossing number at p by referring back to the points of C_1 and C_2 that lie above p. The total complexity is $O(k_1 k_2)$ in time and space.

Assuming now that $\overline{g} = \max_{1 \leq i \leq r} g_i$, the maximum of the genus of the bounding surfaces of the complex K after thickening, it is not hard to verify our claims of time and space complexity for the problems mentioned in Sec. 1. For example, determining the homology class of a cycle of length k involves computing its linking number with each of a generating set of 1-cycles, requiring $O(n\overline{g}k)$ time totally. It is crucial to note though that following the comment in Sec. 2 we need only find a generating set for $H_1(K)$. Finding a basis of $H_1(K)$ could blow up the complexity to $O(n^2\overline{g})$ from $O(n\overline{g})$.

There is considerable scope for further investigation:

- Find tight complexity bounds for the problems considered here. We do not know if our algorithms are optimal, except for ones that are trivially so.
- Find similar algorithms for the homotopy groups. This of course is much harder and one might therefore consider more restricted class of complexes that tend to arise naturally (see [4]).
- Extend these methods of analysis to topological objects, in particular simplicial complexes, in spaces of dimension higher than 3.
- Find applications to real world objects. There seem interesting possibilities. Topology has long been applied in the physical sciences, and currently exciting applications are being found in molecular biology [8, 17].
- See [3, 18] for a survey of related problems in the rapidly growing field of computational topology.

Acknowledgement. We thank Tarun K. Mukherjee, Jadavpur University, Calcutta, for several motivating discussions.

References

[1] C. J. A. Delfinado, H. Edelsbrunner, An incremental algorithm for betti numbers of simplicial complexes, *Proc. 9th ACM Symp. Comp. Geom.*, 1993, 232-239.

[2] T. K. Dey, Optimal algorithms to detect null-homologous cycles on 2-manifolds, *Proc. 5th Canadian Conf. Comp. Geom.*, 1993, 273-278, also *in press*, *Intl. J. Comput. Geom. and Appl.*.

[3] T. K. Dey, Recent developments in computational topology – A survey, *preprint*, 1995.

[4] T. K. Dey, S. Guha, Optimal algorithms for curves on surfaces, *Proc. 32nd IEEE FOCS*, 1995, 266-273.

[5] B. R. Donald, D. R. Chang, On the complexity of computing the homology type of a triangulation, *Proc. 32nd Ann. IEEE Symp. Found. Comp. Sc.*, 1991, 650-661.

[6] H. Edelsbrunner, The union of balls and its dual shape, *Discrete Comput. Geom.* **13** (1995), 415–440.

[7] H. Edelsbrunner, Modeling with simplicial complexes, *Proc. 6th. Canadian Conf. Comput. Geom.*, 1994, 36-44.

[8] H. Edelsbrunner, M. Facello, J. Liang, On the definition and the construction of pockets in macromolecules, *manuscript*, 1995.

[9] H. Edelsbrunner, E. P. Mücke, Three dimensional alpha shapes, *ACM Trans. Graphics* **13** (1994), 43-72.

[10] R. Kannan, A. Bachem, Polynomial algorithms for computing the Smith and Hermite normal forms of an integer matrix, *SIAM Jour. Comp.* **8** (1979), 499-507.

[11] W. S. Massey, *A Basic Course in Algebraic Topology*, Springer-Verlag, 1991.

[12] E. E. Moise, *Geometric Topology in Dimensions 2 and 3*, Springer-Verlag, 1977.

[13] J. R. Munkres, *Elements of Algebraic Topology*, Addison-Wesley, 1984.

[14] F. P. Preparata, M. I. Shamos, *Computational Geometry: An Introduction*, Springer-Verlag, 1985.

[15] D. Rolfsen, *Knots and Links*, Publish or Perish, 1976.

[16] H. Seifert, W. Threlfall, *A Textbook of Topology*, Academic Press, 1980.

[17] D. W. Sumners, Untangling DNA, *Math. Intell.* **12** (1990), 71-80.

[18] G. Vegter, Computational topology, *preprint*, 1995.

[19] G. Vegter, C. K. Yap, Computational complexity of combinatorial surfaces, *Proc. 6th ACM Symp. Comp. Geom.*, 1990, 102-111.

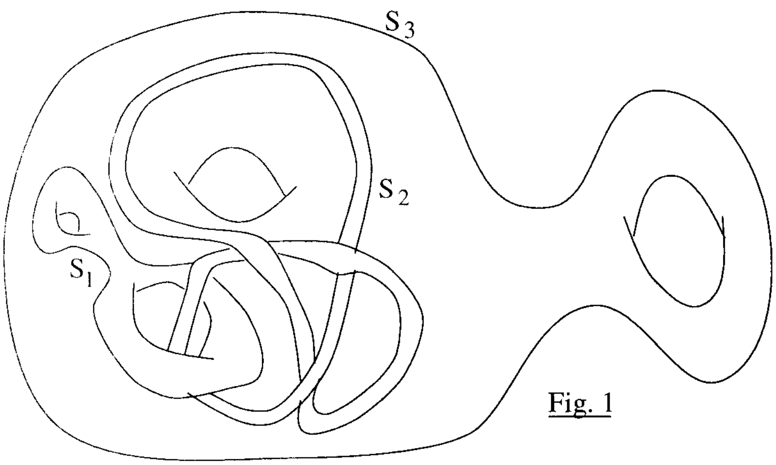

Fig. 1

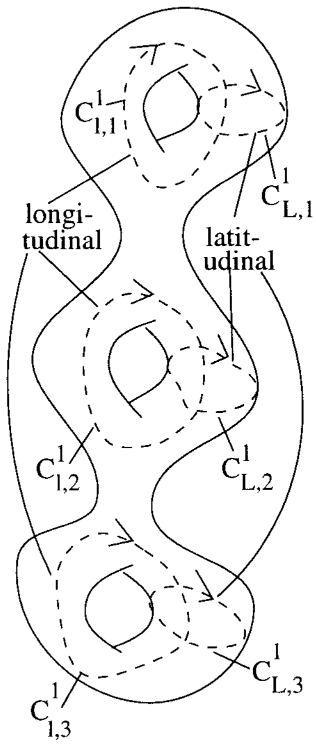

Fig. 2

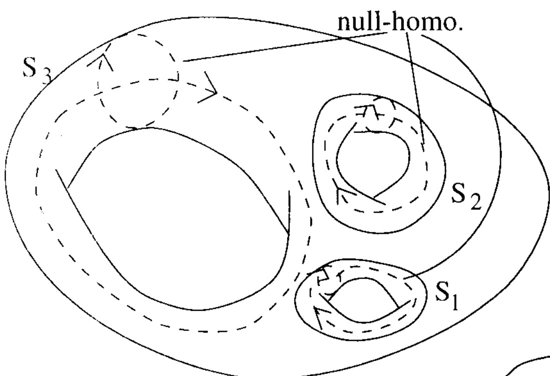

Fig. 3

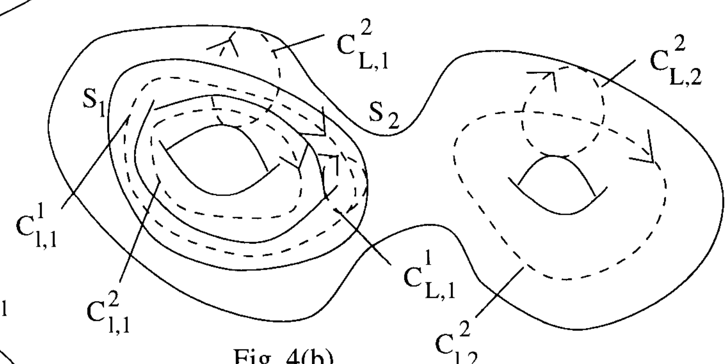

Fig. 4(b)

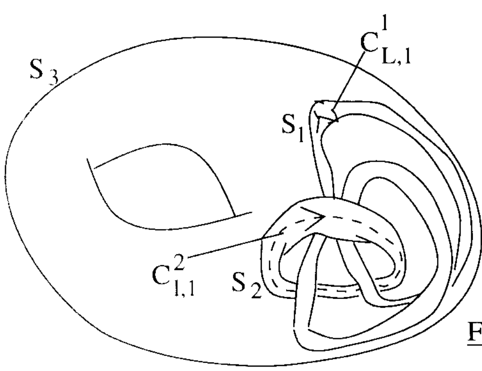

Fig. 4(a)

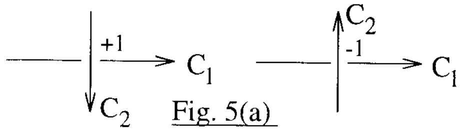

Fig. 5(a)

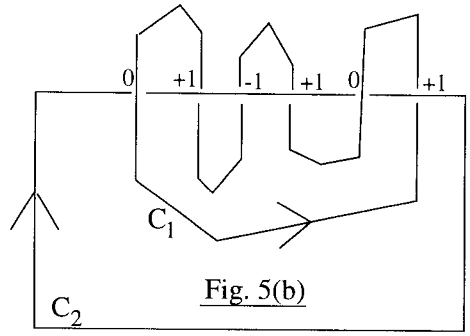

Fig. 5(b)

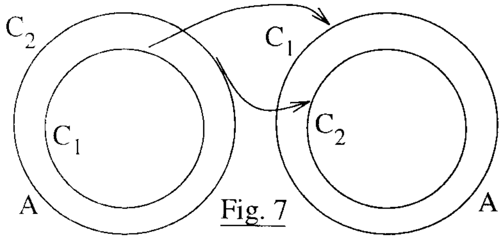

Fig. 7

Fig. 6(a)

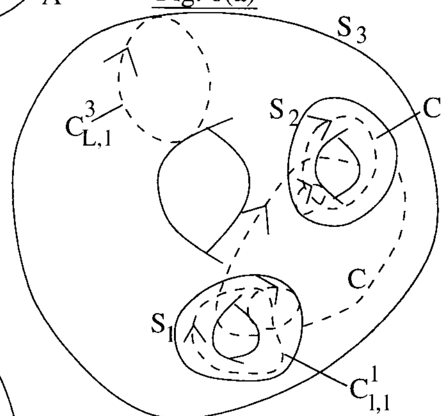

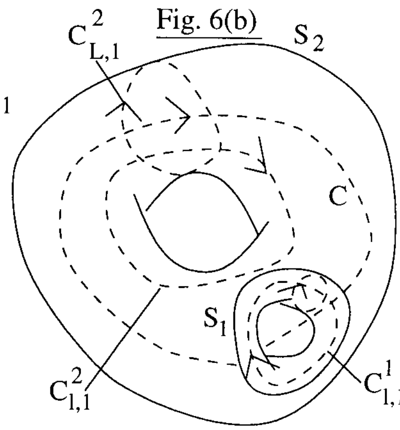

Fig. 6(b)

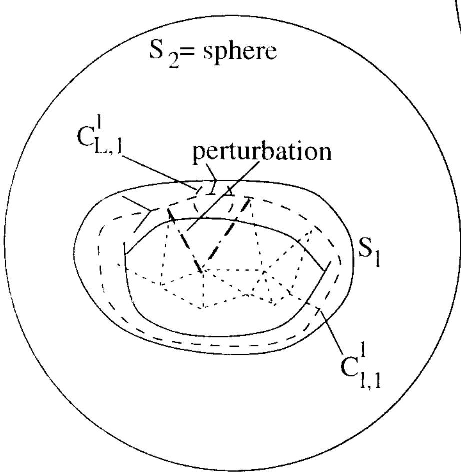

Fig. 8

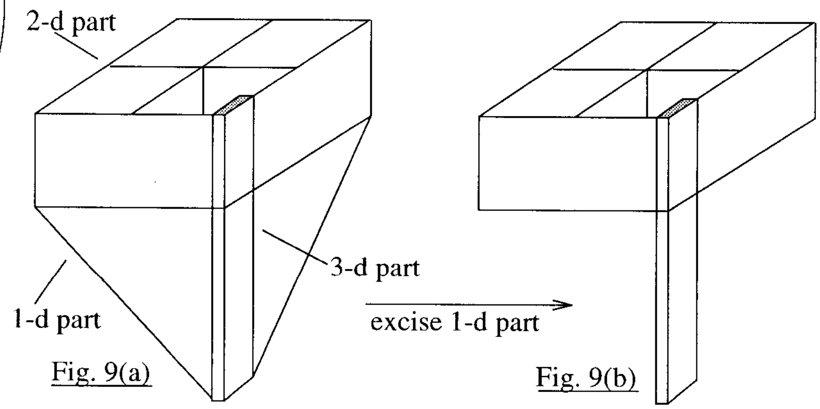

Fig. 9(a)

Fig. 9(b)

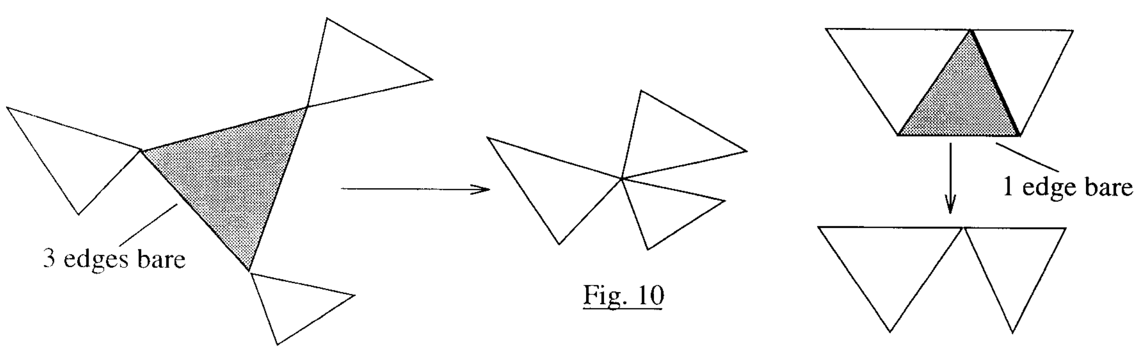

Fig. 10